Desalination and Water Treatment
www.deswater.com

doi: 10.1080/19443994.2015.1044915

57 (2016) 11835–11849
May

Taylor & Francis
Taylor & Francis Group

Heterogeneous Fenton-like oxidation of crystal violet using an iron loaded ZSM-5 zeolite

Burcu Akın Ünnü, Gönül Gündüz, Meral Dükkancı*

Chemical Engineering Department, Ege University, 35100 Bornova, İzmir, Turkey, Tel. +90 5324738874; email: burcuunnu35@gmail.com (B.A. Ünnü), Tel. +90 2323112292; email: gonul.gunduz@ege.edu.tr (G. Gündüz), Tel. +90 2323111493; Fax: +90 2323887776; email: meral.dukkanci@ege.edu.tr (M. Dükkancı)

Received 11 September 2014; Accepted 18 April 2015

ABSTRACT

The heterogeneous Fenton-like oxidation of a cationic triphenylmethane dye, crystal violet (CV), dissolved in water was investigated using an iron-loaded ZSM-5 zeolite catalyst. The catalyst was characterized by powder X-ray diffraction patterns, Fourier Transform infrared spectroscopy (FTIR), scanning electron microscope, analysis, and nitrogen adsorption-Brunauer-Emmet-Teller (N_2-BET) studies. The effects of temperature, solution pH, H_2O_2 amount, catalyst amount, and initial dye concentration were investigated using the heterogeneous Fenton-like oxidation of an aqueous CV. The increase in the concentration of H_2O_2 from 3 to 7.5 mM enhanced the decolorization. Whereas increasing the H_2O_2 amount from 7.5 to 10 mM led to a decrease in the color removal from 94.1 to 85.5%. An acidic pH of 3.5 was favorable for the decolorization of the dye. The decolorization of the dye decreased with the increase in the initial concentration of CV. Doubling the amount of the catalyst enhanced the decolorization from 94.1 to 99.6% while the chemical oxygen demand (COD) removal changed from 50 to 58.8%. The increase in temperature positively affected the decolorization and the COD reduction of the dye. The stability of the catalyst was maintained even after using the catalyst for three cycles, and a small iron leaching was also proof of the stability of the catalyst. The initial color removal rate of the CV was described as $-r_{CV,o} = 7.3\ e^{-14.7/RT}\ C_{CV,o}{}^{0.7}\ C_{H_2O_2,0}$ where $R = 8.314$ J/mol K and $C_{CV,o}$ and $C_{H_2O_2,0}$ were in mol/dm^3.

Keywords: Advanced oxidation process; Heterogeneous Fenton-like oxidation; Crystal violet; Iron-loaded ZSM-5 Zeolite catalyst

---

1. Introduction

The wastewater from textile, dyeing, printing, and other related industries has long been a major environmental problem all over the world. It is estimated that over 100,000 synthetic dyes are available in the world, and almost 7×10^5 tons of dye stuff are produced annually. Colored wastewater streams could pose serious detrimental effects to the environment and thus to human health. Hence, these effluents must be treated or decolorized prior to discharge [1].

A wide range of methods has been developed for the removal of synthetic dyes from water. The techniques can be classified with three categories: chemical, physical, and biological. Biological treatment

---

*Corresponding author.

technologies are insufficient for the decolorization of textile wastewater and the color remains due to the nonbiodegradable nature of the chromophoric groups. Physical treatment technologies, such as coagulation/flocculation, adsorption (mainly on activated carbon), and membrane processes, can result in successful removal of color from the effluent, however, the disadvantage of these methods is the existence of another form of waste for example solid waste such as spent carbon or sludge [2,3]. Among all the other methods, the oxidation processes are found to be very effective which is dependant on the type of oxidant, structure of the catalyst, and chemical composition.

This study presents the catalytic behavior of an iron-loaded ZSM-5 zeolite in the heterogeneous Fenton-like oxidation of crystal violet which is a cationic triphenylmethane dye. Crystal violet is widely used in animal and veterinary medicine as a biological stain and for identifying bloody fingerprints. It is also extensively used in textile dying and paper colorization. Crystal violet is harmful by inhalation, ingestion, and skin contact and also has been found to cause cancer and severe eye irritation in human beings. It is also a mutagen and a mitotic poison [4,5].

Up to now, degradation of crystal violet (CV) was studied using several advanced oxidation processes (AOPs) such as: heterogeneous oxidation with H_2O_2 over copper(II) amine complexes supported on Amberlyst-15 [6], photocatalytic degradation in the presence of Ag^+ doped TiO_2 or nanostructured TiO_2 ultrafine powder or silver doped TiO_2 catalysts, homogeneous, and heterogeneous Fenton reaction, in the presence of bulk CdS, nano-CdS, nano-CdS/zeolite A, and CdO/zeolite and P25-TiO_2 catalyst [1,4,7–13], electrochemical oxidation using a boron-doped diamond or Ti/RuO_2-IrO_2 anode [14,15], electrocoagulation using iron or aluminum electrodes [16], wet peroxide oxidation in the presence of FeGAC/H_2O_2 [17], degradation with a magnetic $CuFe_2O_4$ aqueous solution coupled with microwave radiation [18], and a photocatalytic-biological system combination [19]. In addition, mineralization or chemical oxygen demand (COD) removal data have been reported in a few studies for CV degradation. A COD removal of 85, 70, and 46% was obtained for 20, 40, and 60 ppm CV after 105 min of oxidation by photocatalytic degradation on silver ion doped TiO_2 [4]. A 91.9% TOC removal was obtained in 1 h the by homogeneous Fenton-like oxidation of CV [10]. A TOC removal of 65% was achieved in 300 min by the photocatalytic decolorization of CV in an aqueous nano-ZnO suspension under visible light [20].

In recent years, the AOPs have received considerable attention for the destructive oxidation of dyes and textile effluents, since many aromatic compounds have proven to be degraded effectively to CO_2, H_2O, and small molecules [21].

The most widely known AOPs include heterogeneous catalytic oxidation, heterogeneous photocatalytic oxidation, treatment with ozone in basic and acidic media (often combined with hydrogen peroxide, ultraviolet (UV) light or both hydrogen peroxide/UV systems), and the Fenton and photo-Fenton reactions.

The classical Fenton's reagent allows higher oxidation efficiencies (up to 95%) under mild conditions ($T < 50^\circ C$, 0.1–0.3 MPa), using hydrogen peroxide and a homogeneous Fe^{2+} catalyst.

The Fenton reaction based on ferrous ion is as follows:

$$Fe^{2+} + H_2O_2 \rightarrow Fe^{3+} + {}^{\bullet}OH + OH^- \quad (k = 63\ M^{-1}\ s^{-1}) \tag{1}$$

Iron (III) can then react with hydrogen peroxide in the so-called Fenton-like reaction (Eqs. (2)–(4))

$$Fe^{3+} + H_2O_2 \rightleftarrows FeOOH^{2+} + H^+ \, (k = 10^{-3}–10^{-2}\ M^{-1}\ s^{-1}) \tag{2}$$

$$FeOOH^{2+} \rightarrow HO_2^{\bullet} + Fe^{2+} \tag{3}$$

$$Fe^{3+} + HO_2^{\bullet} \rightarrow Fe^{2+} + O_2 + H^+ \quad (k = 1x10^4\ M^{-1}\ s^{-1}) \tag{4}$$

Fenton's process may not be applicable to alkaline solutions or sludges with strong buffering capacities. Another disadvantage of Fenton's treatment is the production of iron sludge, which must be disposed of [22–24]. Under these circumstances, there is a need for heterogeneous catalytic procedures where the catalyst is in a different phase and, in particular, zeolites, whose recovery from water and regeneration, are not too difficult [25,26]. Fe-loaded zeolites show redox properties because iron can change its oxidation state in the presence of H_2O_2, Eq. (2). While the rate of Eq. (2) is much smaller than that of Eq. (1) with which hydroxyl radicals are formed, to enhance the reduction of Fe^{3+} to Fe^{2+} on the surface of the catalyst, reducing agents such as ascorbic acid, and hydroxylamine, humic acid, or UV-light can be used [27–30]. These materials are effective catalysts for the oxidative breakdown of phenol [31,32], a number of carboxylic acids [33], and ethanol [34] in water. In addition to these, Fe-loaded ZSM-5 zeolite catalysts were used efficiently for decolorization of different kinds of dyes such as Orange II [35–37], anthraquinone dye Reactive Brilliant Blue KN-R [38], Rhodamine 6G [39–42], and Reactive Red 141 [43]. The use of hydrogen peroxide as an oxidant is also helpful, since no additional pressure is required, as in the case of gaseous oxidants, such as O_2 or O_3. The use of heterogeneous catalysts is a very promising way to treat wastewater streams as it permits treatment under mild temperature and pressure conditions without the necessity of catalyst recovery as required with homogeneous catalysis [44].

In light of this literature survey, heterogeneous Fenton-like oxidation was chosen as the AOP to degrade crystal violet. On the other hand, to the best of our knowledge, no study has been reported in literature on the heterogeneous Fenton-like degradation of CV in the presence of a FeZSM-5 zeolite catalyst. In this study, the aim was to investigate the influence of several parameters such as temperature, solution pH, the H_2O_2 amount, catalyst amount, and initial dye concentration on the heterogeneous Fenton-like degradation of CV using an iron-loaded ZSM-5 zeolite catalyst.

2. Experimental study

2.1. Materials

The crystal violet (CV) dye was purchased from Merck (Germany) and used without any purification. The absorption spectra of CV are characterized by two main bands, one in the visible region ($\lambda_{\max} = 590$ nm) which is responsible for the chromophoric components and the other in the UV region ($\lambda_{\max} = 300$ nm). In this study, the decay in the band at 590 nm was investigated as a function of time as a measure of the decolorization degree.

The hydrogen peroxide solution (35% in mass) of analytical grade was also obtained from Merck. All aqueous solutions were prepared with water obtained from a Millipore Direct Q purification unit. The chemical structure of CV is given in Fig. 1.

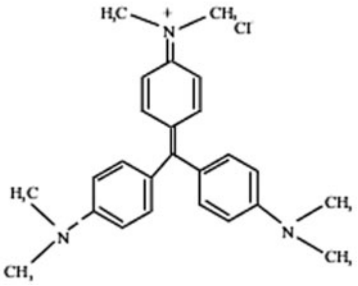

Fig. 1. Chemical structures of CV.

2.2. Catalyst preparation

In this study, a FeZSM-5 (42) catalyst was prepared by the ion exchange method used by Schwidder et al. [45]. The method was applied with small differences. For this purpose, 5 g of the parent ZSM-5 zeolite (Si/Al = 42), 1.825 g of Fe powder (Riedel-de Haen AG), and 500 cm^3 of deionized water were charged into a double-necked flask equipped with a gas inlet tube and a magnetic stirrer. After the flask was flushed with nitrogen (in the study of Schwidder et al. [45] argon was used) for 3 min, 4.14 cm^3 of concentrated hydrochloric acid (37% in mass, J.T. Baker) was slowly added to the mixture. The liquid was stirred under nitrogen atmosphere for 5 d. Ferrous ions are easily oxidized to corresponding ferric ions by oxygen in air; the presence of nitrogen prevents this oxidation. So, a pure Fe^{2+} solution could be obtained by reaction between the iron powder and hydrochloric acid solution under the atmosphere of inert N_2 gas. After 5 d, it was filtered, and the obtained FeZSM-5 (42) sample was washed with deionized water until no Cl^- was detected in the washing water. The catalyst was dried at room temperature and calcined.

For calcination, the catalyst was first heated to 423 K at a rate of 80 K/min and kept at 423 K for 15 min and then heated to 873 K at a rate of 47 K/min under air and remained at this temperature for 2 h. It was observed that after the calcination step, the color of the catalyst (light brown) did not change.

2.3. Catalyst characterization

The prepared FeZSM-5 catalyst was characterized by nitrogen adsorption, XRD, scanning electron microscope (SEM), FTIR, and inductively coupled plasma atomic emission spectrometer (ICP-AES) measurements.

Powder X-ray diffraction patterns (XRD) of the catalyst were recorded in the range of 5–70° using a Shimadzu 6000 XRD with Cu-Kα radiation to determine the crystalline structure of the sample, and the morphological properties were analyzed with a SEM (FEI Quanta 250 FEG SEM). Nitrogen adsorption isotherms at 77 K were measured using nitrogen adsorption (Micromeritics ASAP 2010) equipment. The FT-Infrared spectra were recorded in the 4,000–650 cm^{-1} with a Perkin–Elmer Spectrum 100 FTIR. The iron content of the catalyst was determined with the Varian-96 ICP-AES using the fusion dissolution method.

2.4. Experimental procedure

The oxidative degradation of CV was performed under isothermal conditions (323 K) in a shaded temperature-controlled glass batch reactor equipped with a mechanical stirrer at about 280 rpm (Heidolph) and a pH electrode (Mettler Toledo). The experimental set-up used for the catalytic activity tests is illustrated in Fig. 2. In a typical run, 0.15 dm^3 of aqueous dye solution with a known concentration was placed into the reactor and the temperature was adjusted to 323 K. When the temperature reached 323 K, the pH of the solution was measured and 0.15 g of catalyst (1 g/dm^3) was added to the solution with continuous stirring. After stirring for 10 min, the pH of the solution was again measured. Then, a solution of 35% H_2O_2 with a known concentration was added to the solution. After stirring for 3 min, the pH of the solution was again measured and this time was recorded as the starting time of the reaction. All the runs (except the run for the effect of solution pH on the dye degradation) were started at the dye initial pH of 7. No attempt was made to change the solution pH during the runs. The samples taken periodically at every 15 min were placed in an ice bath to quench the reaction and then centrifugated for 30 min to remove the catalyst. After that, the samples diluted with water at a 1:5 ratio were analyzed with a UV spectrophotometer (Jasco 7800 UV/Vis) at 590 nm. The decrease of the intensity of the band at 590 nm was used as a measure of decolorization degree. One run took 2 h. The extent of the decolorization of the aqueous solution of CV was calculated as a function of time using the initial absorbance and absorbance for the corresponding time.

In addition to these measurements, the reduction in the COD of the dye solution was determined by measuring the initial COD and final COD (after oxidation for 2 h) of the aqueous dye solution with a Lovibond Checkit Direct COD Vario device.

3. Results and discussion

3.1. Catalyst characterization

3.1.1. XRD studies

The XRD patterns of the catalyst and parent ZSM-5 zeolite are given together for comparison in Fig. 3. All samples exhibited the typical diffractograms of the ZSM-5 zeolite (MFI framework) ($2\theta = 7–9^\circ$ and 23–25°) given in literature [25,32,34,46–53]. It emphasized that the high dispersion of Fe ions in the compensating positions inside the zeolites did not damage the crystallinity of the zeolite. The observed decrease in the peak intensities of the FeZSM-5 (42) catalyst may arise from the enhanced absorption of X-rays due to iron cations and to the reduction in the crystal size of the zeolite as a result of the acid treatment step. The course of the baseline indicates that no impurity phase was observed.

3.1.2. SEM studies

Fig. 4 indicates the morphology of the prepared FeZSM-5 (42) zeolite sample and parent ZSM-5 zeolite with the scale of ×25,000 (Fig. 4(a) and (c)) or ×50,000 (Fig. 4(b) and (d)). The SEM images of ZSM-5 zeolite (Si/Al = 42) depicted that the crystallites were in spherical form with a diameter of around 500 nm which is in agreement with literature [54]. However, the SEM images of the FeZSM-5 (42) catalyst showed that the crystallites were nonuniform in shape and the incorporation of the iron cations into the zeolite structure could not be clearly seen. The presence of iron cations in the structure of the prepared catalyst was confirmed by ICP-AES analysis, see Table 1.

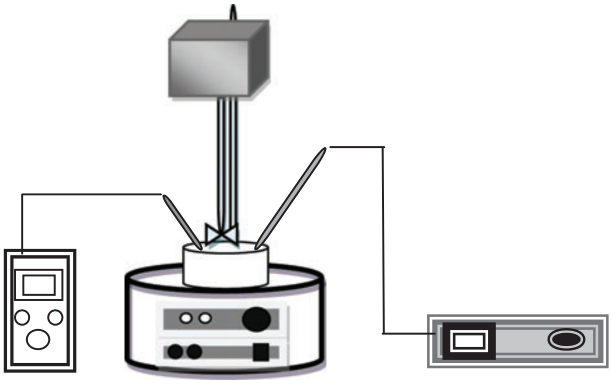

Fig. 2. Experimental set-up used in the heterogeneous Fenton-like oxidation of crystal violet.

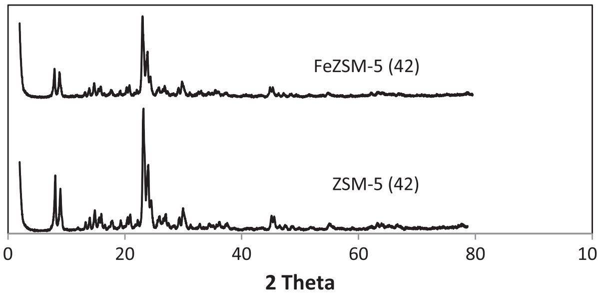

Fig. 3. XRD patterns of prepared FeZSM-5 and parent ZSM-5 zeolite.

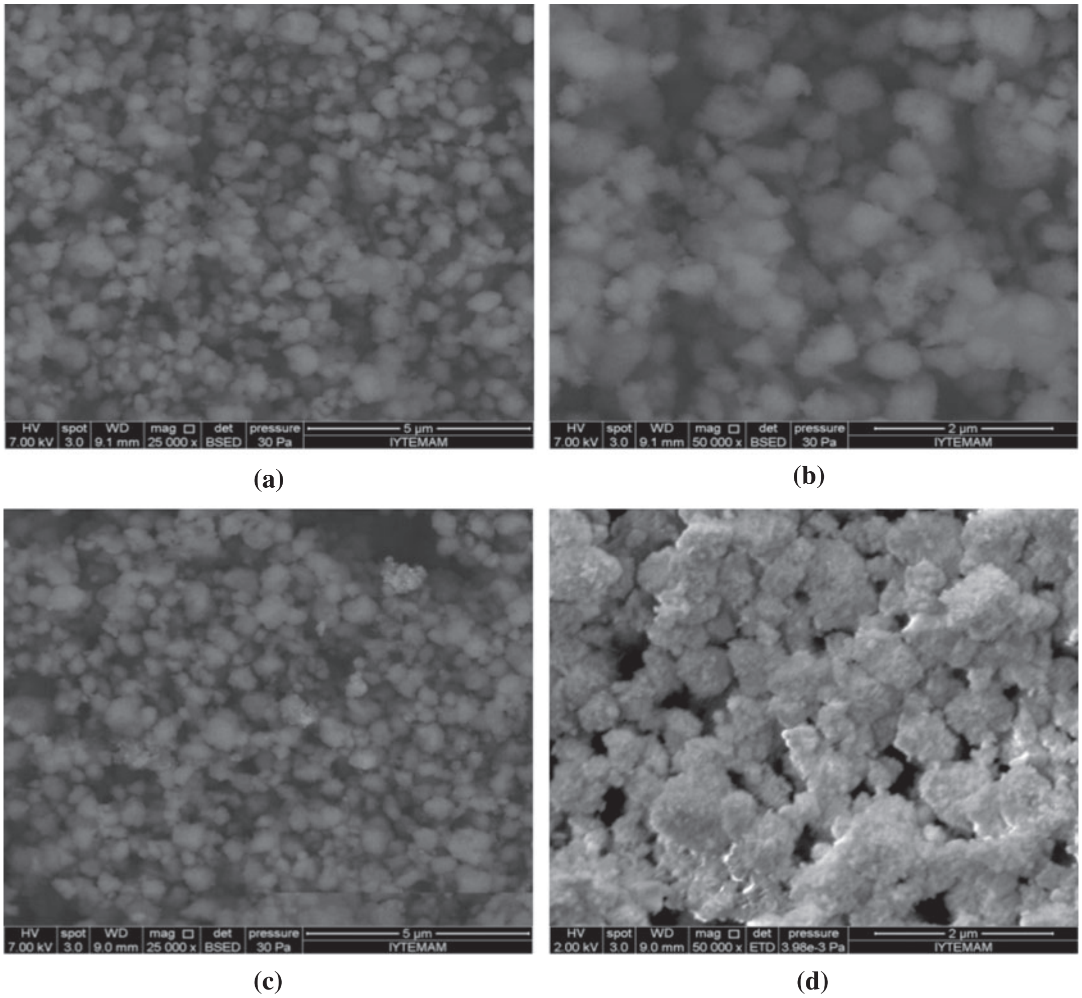

Fig. 4. SEM images of the catalyst prepared by ion exchange and the parent ZSM-5 zeolite (a,b) ZSM-5 (42) and (c,d) FeZSM-5 (42).

Table 1
Some surface characteristics of the prepared catalyst and parent ZSM-5 zeolite

Samples	S_{BET}, (m^2/g)	V_p, (cm^3/g)	V_{μ}, (cm^3/g)	S_{μ}, (m^2/g)	V_{max}, (cm^3/g)	d_{ave}, * (nm)	Iron content, wt.%	Iron content, mol/$g_{zeolite}$
ZSM-5 (42)	378.5	0.1507	0.0796	134.7	193.92	0.98	–	–
FeZSM-5 (42)	368.9	0.1256	0.0898	163.7	201.09	0.59	7	12.5×10^{-4}

*Horvath kawazoe method.

3.1.3. FTIR studies

The FTIR spectra of the parent ZSM-5 zeolite and the corresponding Fe-loaded one are depicted in Fig. 5 in the range of 650–4,000 cm^{-1} and 2,500–4,000 cm^{-1} as inset for FeZSM-5 (42). The broad band in the range of 3,000–3,500 cm^{-1} shows the Fe-OH vibration. The bands at 800, 1,100, and 1,225 cm^{-1} are assigned to different vibrations of the tetrahedral and framework structure of the ZSM-5 zeolite [52,53]. Similar peaks at 805, 1,090, and 1,290 cm^{-1} were observed in a study by Nezamzadeh-Ejhieh and Karimi-Shamsabadi [55] The band at about 1,100 cm^{-1} is due to the internal vibrations of the (Si, Al) O_4 tetrahedral of the ZSM-5, whereas the bands at 1,225 and 800 are due to

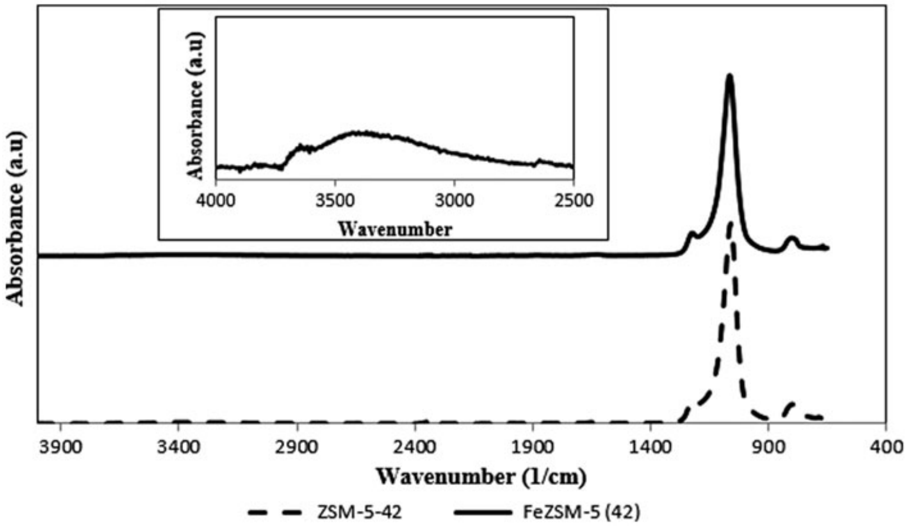

Fig. 5. FTIR spectra of the parent ZSM-5 zeolite and prepared FeZSM-5 catalyst.

vibrations related to the external linkages between the tetrahedral and hence sensitive to the framework structure [30,47,48].

3.1.4. N_2-BET studies

The surface characteristics of the prepared FeZSM-5 (42) catalyst and the parent ZSM-5 zeolite including the BET surface area (S_{BET}), total pore volume (V_{p}), micropore volume (V_{μ}), micropore area (S_{μ}), maximum adsorbed volume ($V_{\max}$), and average pore diameter (d_{ave}) are given in Table 1.

Iron loading to the ZSM-5 (42) zeolite by the ion exchange method leads to a reduction in the BET surface area and in the total pore volume. This may be related to the blockage of some zeolite pores due to the formation of some iron species in the pores [55,56]. However, the decrease in total pore volume is more significant than that in BET area. The nitrogen adsorption isotherms are of type II for the FeZSM-5 (42) and ZSM-5(42) samples according to the IUPAC classification.

The Fe content of the catalyst was measured by the ICP-AES method and found to be 7% (in wt.%). As mentioned in Part "2.2 Catalyst Preparation," during the preparation of the catalyst, a pure Fe^{2+} solution could be obtained by the reaction between the iron powder and hydrochloric acid solution under the atmosphere of inert N_2 gas. However, Fe^{2+} can be oxidized to Fe^{3+} ions during the calcination process of the catalyst in air. The Fe^{3+} ions formed are reduced to Fe^{2+} ions through Eqs. (2)–(4). These ions are used in the formation of $OH^{\cdot}$ radicals (Eq. (1)), which are necessary for the degradation of dye by heterogeneous Fenton-like oxidation.

3.2. Catalytic activity tests

3.2.1. The influence of H_2O_2 concentration on the degradation of CV

The initial concentration of H_2O_2 plays an important role in the Fenton process. The oxidation of dyes by the Fenton process is carried out by the $OH^{\cdot}$ radicals that are directly produced from the reaction of the H_2O_2 and Fe^{2+} (Eq. (1)).

In this study, the influence of the H_2O_2 concentration on the oxidation of CV was investigated at an initial pH around 7.0 (which is the initial pH of dye) for the FeZSM-5 (42) catalyst. Fig. 6 displays the obtained results as a function of time for FeZSM-5 (42). The runs were accomplished using H_2O_2 in the range of 3–10 mM for 0.15 dm^3 of 0.025 g/dm^3 dye solution at 323 K for a catalyst amount of 0.15 $g/0.15\ dm^3$ of solution.

A blank experiment was accomplished to determine the adsorption of the CV dye on the zeolite surface. For this purpose, only a catalyst amount of 0.15 g was added to the 0.15 dm^3 of dye solution under continuous stirring. A decolorization of 11.4% was observed due to the adsorption by the catalyst after a reaction time of 2 h in the absence of H_2O_2. As seen in Fig. 6(a), in the presence of H_2O_2 (7.5 mM) only, a color removal of 38.9% was achieved. However, a color removal of 76.2% was achieved after 2 h of oxidation with the combined use of H_2O_2 (3 mM) and

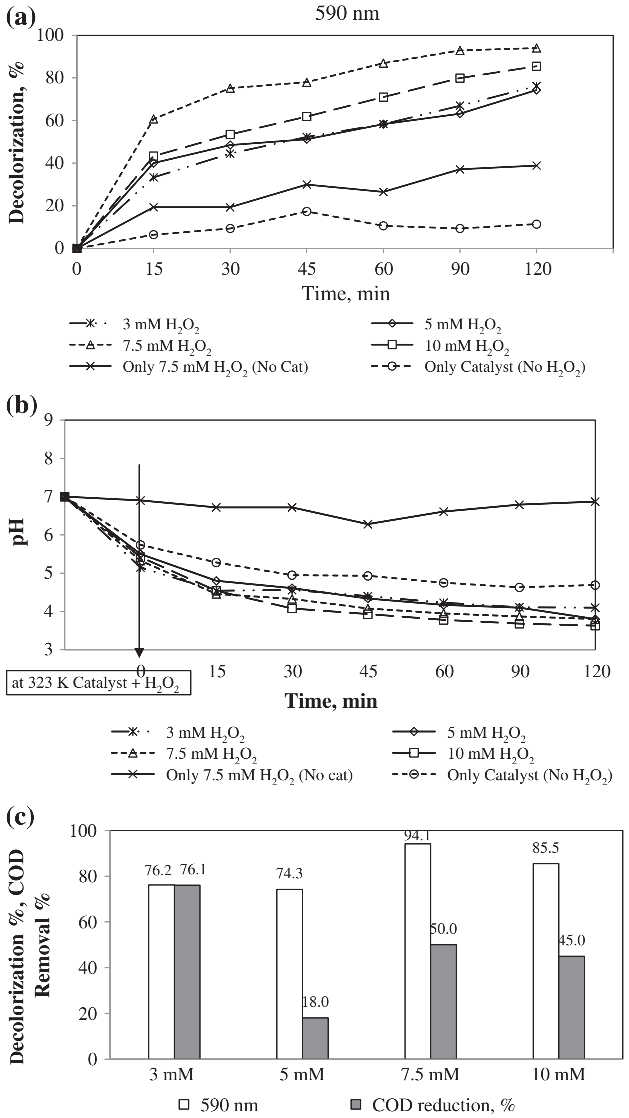

Fig. 6. The effect of the H_2O_2 concentration on the oxidation of CV. (a) Percentage of decolorization as a function of time, (b) pH change as a function of time, and (c) percentage of color removal and COD reduction after 2 h (0.025 g/dm^3 and 0.15 dm^3 CV solution, with 0.15 g catalyst at 323 K, and at a initial pH 7).

the catalyst. This result indicates the efficiency of the heterogeneous Fenton-like process in CV degradation. The increase in H_2O_2 concentration from 3 mM to 5 mM did not significantly affect the color removal after 2 h of oxidation. A slight increase in the initial rate of color removal was observed from 1.36×10^{-6} mol/dm^3 min to 1.63×10^{-6} mol/dm^3 min. When the H_2O_2 concentration was enhanced to 7.5 mM, a drastic increase in color removal of 94.1% was obtained. This result is expected because more OH radicals are produced with the increasing amount of H_2O_2. The increase in H_2O_2 concentration from 7.5 to 10 mM negatively affected the color removal. An excess of H_2O_2 will react with the $OH^{\cdot}$ radicals competing with the organic pollutants and consequently reduce the efficiency of the treatment, namely, the H_2O_2 itself contributes to the OH radical scavenging capacity, Eq. (5).

$$H_2O_2 + OH^{\cdot} \rightarrow HO_2^{\cdot} + H_2O \tag{5}$$

The oxidation potential of the $HO_2^{\cdot}$ radicals is much smaller than that of the $OH^{\cdot}$ species. On the other hand, oxygen and water may be formed by the decomposition of H_2O_2, Eq. (6) [57]:

$$2H_2O_2 \rightarrow 2H_2O + O_2 \tag{6}$$

However, other side reactions relating to the regeneration of H_2O_2 may also occur:

$$2\,HO_2^{\cdot} \rightarrow H_2O_2 + O_2 \tag{7}$$

$$2\,HO^{\cdot} \rightarrow H_2O_2 \tag{8}$$

The regeneration of H_2O_2, as shown in Eqs. (7) and (8) helps the scavenging effect of H_2O_2 to become dominant, as well.

Similar results were reported in literature by Jana et al. [1], by Zhang et al. [15], and by Alshamsi et al. [9] in the oxidation of CV using several advanced oxidation techniques.

During the runs, as the reaction proceeds, organic acids may be formed which lead to a drop of the solution pH (Fig. 6(b)) [40].

The highest COD reduction reached was 76.1% in the presence of 3 mM H_2O_2, but the highest decolorization degree of 94.1% was achieved in the presence of 7.5 mM H_2O_2, Fig. 6(c).

3.2.2. *Influence of pH on the degradation of CV*

The aqueous pH has a major effect on the efficiency of Fenton's treatment. It is well known that Fenton and Fenton-like reactions have a maximum catalytic activity at a pH of about 3–4 [49,50]. In highly acidic conditions, H_2O_2 is stabilized and this inhibits the production of the intermediate ion HO_2^-, which reacts with Fe^{3+} to produce $Fe\text{-}OOH^{2+}$. The latter decomposes to produce Fe^{2+}, which is necessary for the reaction in Eq. (1) in order to generate hydroxyl radicals [58]. At a high alkali pH, H_2O_2 loses its oxidizing potential. The formation of ferrous and ferric oxyhydroxides with pH values of more than 4.0 inhibits the reaction between the Fe^{2+} and H_2O_2. Therefore, the low amount of $OH^{\cdot}$ radical generation can be the reason for low degradation. Also, at a high pH, H_2O_2 decomposes to oxygen [59].

In this study, the effect of pH on the heterogeneous Fenton-like oxidation of CV was investigated at an initial pH of 7 and 3.5. In the run at initial pH of dye (pH = 7), experiment was started at dye pH and no attempt was made to change the solution pH during the run. In the run at pH = 3.5, the catalyst was added to the solution and then pH dropped to 3.5 by the addition of 0.1 N H_2SO_4 to the dye solution and lastly H_2O_2 was added. After that, no attempt was made to change the solution pH during the run. The runs were performed at 323 K using 0.15 dm^3 of 0.025 g/dm^3 dye solution, 7.5 mM H_2O_2, and 0.15 g of catalyst.

As seen in Fig. 7(a), the reduction of the pH to around 3.5 positively affected the color removal. The color removal increased slightly from 94.1 to 99.4% with the decrease of the pH from 7.0 to 3.5; as a result, the low pH accelerated a bit the oxidation of CV due to the formation of more Fe^{2+} from Fe^{3+} present in the structure of zeolite through Eqs. (2)–(4) [39,60].

As seen in Fig. 7(b), when a catalyst was added into the aqueous dye solution, the pH decreased from 7 to about 5 because of the acidity of the catalyst. During the progress of the reaction, pH continued to decrease likely due to the formation of acidic intermediates.

The observed COD reduction for a pH around 3.5 was measured as 53.8% while it was 50% at a pH around 7 (Fig. 7(c)). As seen, no drastic change in color and COD removal was obtained with decreasing pH. This result indicates clearly that the applied pH can be expanded to neutral pH in the heterogeneous Fenton-like oxidation of CV. The slight decrease in discolorization and COD removal observed at dye initial pH of 7 may be likely due to the accelerated formation of less reactive $HO_2^{\cdot}$ radicals rather than $OH^{\cdot}$ radicals. In addition to this, when the pH of the solution under treatment is much higher than the pK_a, pH influences the degradation insignificantly. The pK_a values of CV are 1.2 and 1.8 [61] which are well below the studied pH values of 3.5 or 7.0. A similar result was also obtained in the catalytic wet peroxide oxidation of Rhodamine G dye in the presence of Fe-exchanged zeolites [42].

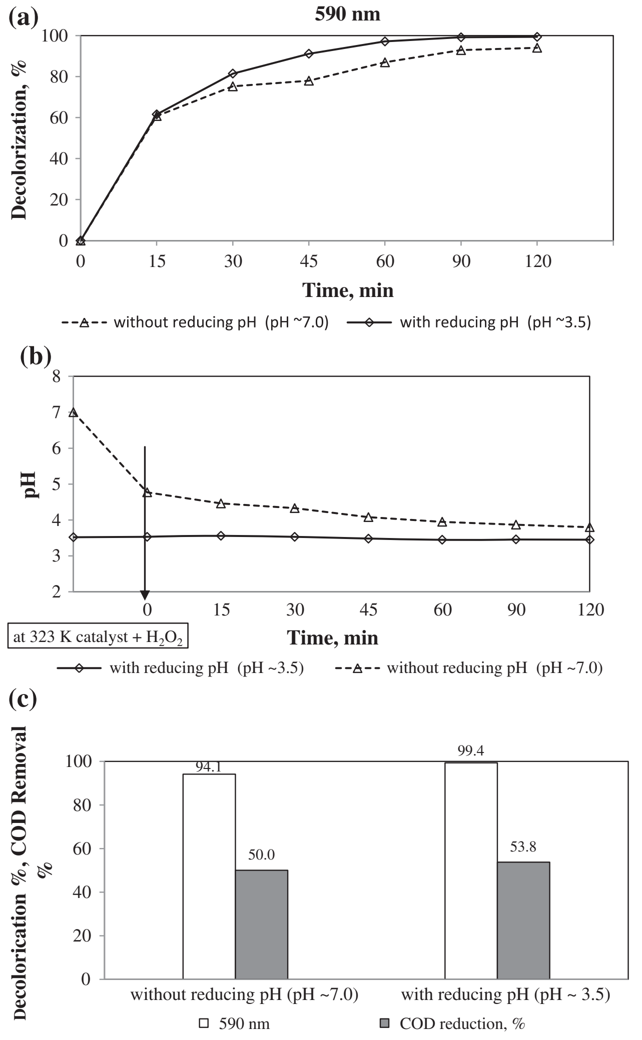

Fig. 7. Heterogeneous Fenton-like oxidation of CV with and without regulation of pH. (a) Percentage of decolorization as a function of time, (b) pH change as a function of time, and (c) percentage of color removal and COD reduction after 2 h (0.025 g/dm^3 and 0.15 dm^3 CV solution with 0.15 g catalyst, and 7.5 mM H_2O_2 addition at 323 K).

Different results are presented in literature on the effect of pH on the decolorization of CV; Alshamsi et al. [9] reported that dye decolorization was not affected in an acidic media in the photocatalytic degradation of CV. In contrast to this result, Nezamzadeh-Ejhieh and Banan [11] found that the maximum decolorization efficiency was obtained in an alkaline pH of 9 in the photodecolorization of CV catalyzed by CdS nano particles. Chen et al. [17] revealed that granular activated carbon (FeGAC)/H_2O_2 had better removal efficiency at a pH of 3 than at a pH of 6. Sahoo et al. [4] showed that the dye degradation varied only by 2% with a pH change between 3 and 11 in the photocatalytic degradation of CV on silver ion doped TiO_2. In another study, the removal of CV by adsorption on a surfactant (sodium dodecyl sulfate, SDS)-modified alumina increased with the increase of the pH to 8, and then, it gradually decreased [62]. The CV removal extent increased by adsorption on palm kernel fiber from 79.1% at a pH of 2.4–87.5% at a pH of 7.0 [63].

3.2.3. Influence of initial concentration of CV on degradation

The effect of the initial concentration of dye was studied by varying the initial concentration of dye between 0.005 and 0.035 g/dm^3 with a constant H_2O_2 concentration of 7.5 mM, a constant catalyst amount of 0.15 g/0.15 dm^3 solution (1 g/dm^3), at 323 K for 2 h of oxidation. Fig. 8 presents the percentages of decolorization as a function of time. The initial decolorization rate increased slightly with decreasing initial concentration of CV except for 0.005 g/dm^3. A drastic increase in the initial rate of color removal was observed when 0.005 g/dm^3 dye was used. Color removal decreased from 98.4 to 90.8% after 2 h of oxidation with the increase in the initial concentration of dye from 0.005 to 0.035 g/dm^3. The decrease in color removal with increasing dye concentration can be attributed to the hydroxyl radicals formed less than the required amount for high dye concentration. A similar trend was observed by Sahoo et al. [4] in the photocatalytic degradation of CV on silver ion doped TiO_2.

On the other hand, almost the same COD removal, 33.3 and 32.0%, was obtained for 0.005 and 0.015 g/dm^3 of CV concentration, respectively. But an increase in the COD to 50.0% was observed when 0.025 g/dm^3 dye was used. The decolorizaton rate of the dye is directly proportional to the possibility of the formation of hydroxyl radicals on the zeolite surface, Eq. (1), and then probability of the reaction of these hydroxyl radicals with the dye molecules. The lifetime of hydroxyl radicals is about a few nanoseconds, and thus, they can only react with the dye molecules where they are formed. Increasing the dye concentration per unit volume may enhance the possibility of collision between dye molecules and the hydroxyl radicals, causing the increase in the mineralization efficiency [64–67]. However, in a rather high concentration of dye, the $OH^{\cdot}$ radical concentration would not be high enough to react with the dye molecules, resulting in the decrease of COD removal, as obtained with dye concentration of 0.035 g/dm^3.

Alshamsi et al. [9] showed that the apparent rate constant for the first order decolorization decreased as the dye concentration increased. A similar trend in the rate constant with an increasing initial concentration of dye was observed in our study, as seen in Fig. 8(c). The first order rate constant decreased drastically when the concentration of dye increased from 0.005 to 0.015 g/dm^3, whereas at concentrations higher than 0.015 g/dm^3, a slight decrease in the rate constants was observed.

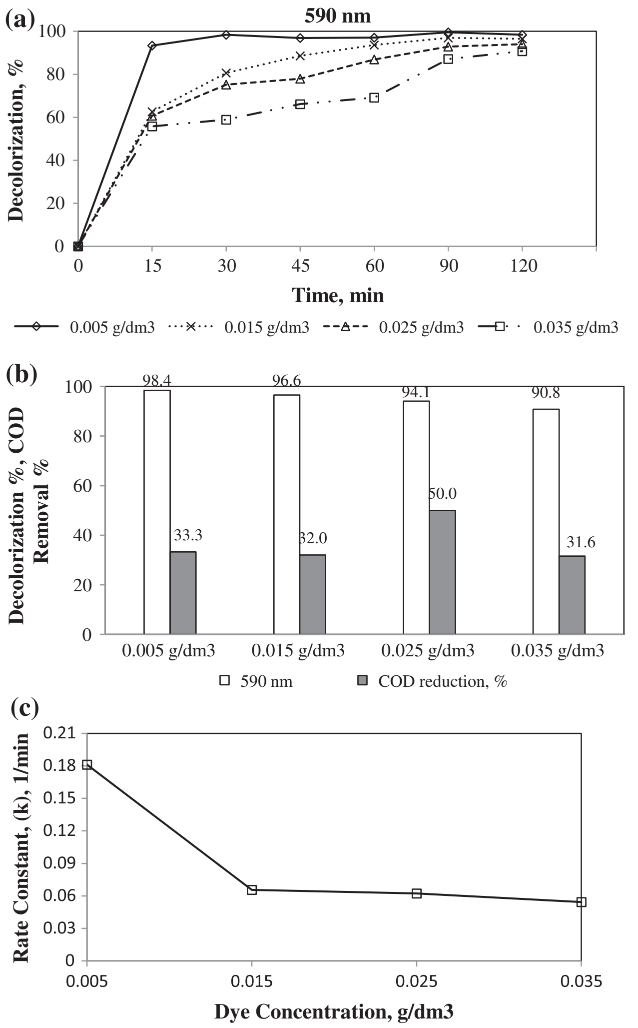

Fig. 8. Catalytic oxidation runs with different initial dye concentrations (a) percentage of decolorization as a function of time, (b) percentage of color removal and COD reduction after 2 h, and (c) change of rate constant with the initial concentration of dye (with first order assumption; 0.15 dm^3 CV solution, with 0.15 g catalyst, and 7.5 mM H_2O_2 addition at 323 K).

3.2.4. Effect of catalyst amount on the degradation of CV

The influence of the catalyst concentration on CV removal was studied using catalyst amounts of 0.15 and 0.3 g for 0.15 dm^3 dye solution under the following reaction conditions: initial CV concentration of 0.025 g/dm^3, temperature of 323 K, 7.5 mM H_2O_2, and an initial pH 7.0. The results are presented in

Fig. 9. A doubled amount of catalyst increased the initial decolorization rate from 2.5×10^{-3} to 3.9×10^{-3} mmol/dm^3 min while the color removal changed from 94.1 to 99.6% (almost complete color removal) after a reaction time of 2 h (Fig. 9(a)).

For both cases, the initial pH of the aqueous dye solution decreased from 7 to about 3.9 in the reaction duration due to the formation of acidic intermediates (Fig. 9(b)).

The COD reduction increased with the increasing amount of catalyst from 50 to 58.8%, which may arise from the increase in the active sites of the catalyst, Fig. 9(c).

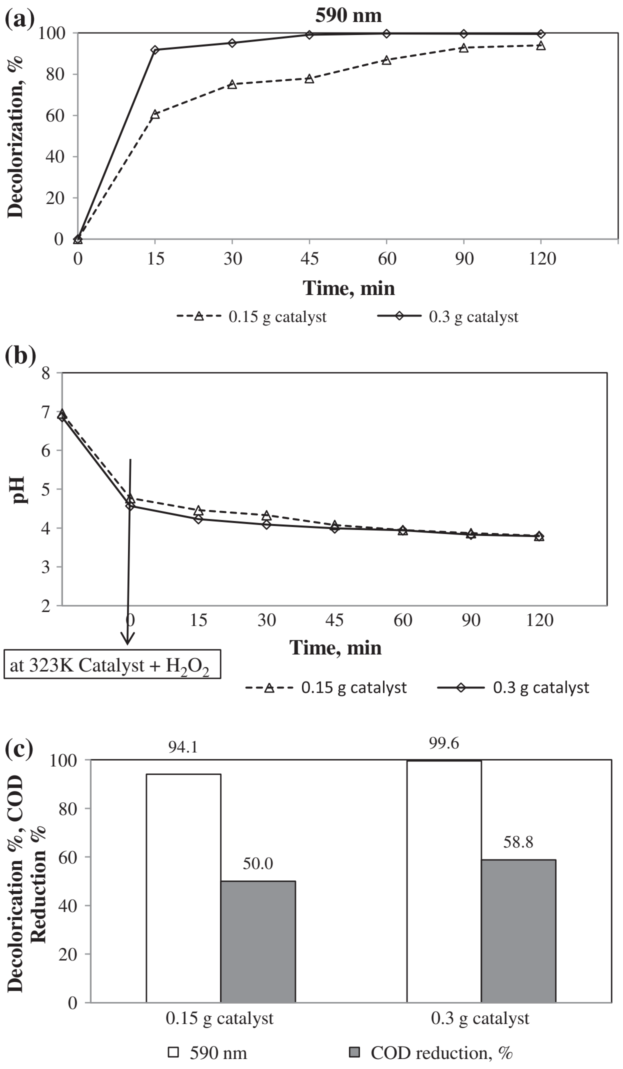

Fig. 9. Catalytic oxidation runs with different catalyst amounts at an initial pH around 7.0. (a) Percentage of decolorization as a function of time, (b) pH change as a function of time, and (c) percentage of color removal and COD reduction after 2 h (0.025 g/dm^3 and 0.15 dm^3 CV solution, 7.5 mM H_2O_2 addition at 323 K).

The increase in the degradation of CV with the increase in catalyst dose was reported by Sahoo et al. [4] in the photocatalytic degradation of CV on Ag^+ doped TiO_2, and by Nezamzadeh-Ejhieh and Banan [11] in the sunlight assisted photodecolorization of CV catalyzed by CdS nano particles.

3.2.5. *Effect of temperature on catalytic activity*

Experiments were conducted to investigate the effect of temperature on the degradation of aqueous CV dye solution at four different temperatures, 303, 313, 323, and 333 K under the following conditions; a CV initial concentration of 0.025 g/dm^3, a catalyst amount of 0.15 g/0.15 dm^3 dye solution, at an initial dye pH, and an H_2O_2 amount of 7.5 mM. The results are shown in Fig. 10. The results show clearly that the color removal and initial color removal rate increased with increasing the temperature from 303 K through 323 to 333 K. It was expected due to the exponential dependency of the rate constant with the reaction temperature. A complete color removal was achieved at 333 K after 1 h of reaction.

The solution pH decreased with increasing temperature, as well. It indicated that the formation of acidic intermediates was enhanced with the temperature (Fig. 10(b)).

The lowest decolorization degree was measured at 303 K to be 69.6% after 2 h of oxidation. The reduction of COD increased with temperature resulting in 25.4% at 303 K and at 313 K, 50% at 323 K, and 71.2% at 333 K (Fig. 10(c)).

The enhancement in decolorization efficiency by increasing the temperature was also reported in literature [6,11].

However, high temperature causes significant evaporation of the solution during the experiments, accelerates the decomposition of H_2O_2 into oxygen and water, and decreases the solubility of the O_2 formed. O_2 is also an oxidant, but it is less reactive than OH radicals. Thus, temperatures higher than 333 K are not recommended.

When the results obtained in this study were compared with other Fenton reaction studies in literature for CV, it was seen that almost complete color removal was achieved in the degradation of CV at 298 K for an initial dye concentration of 100 mg/dm^3 in the presence of 1,000 mg/dm^3 H_2O_2 and 100 mg/dm^3 $FeSO_4.7H_2O$ after an oxidation time of 90 min by homogeneous Fenton reaction followed by microfiltration [1].

Heterogeneous Fenton-like oxidation of CV in the presence of FeGAC/H_2O_2 [17] was studied, and the

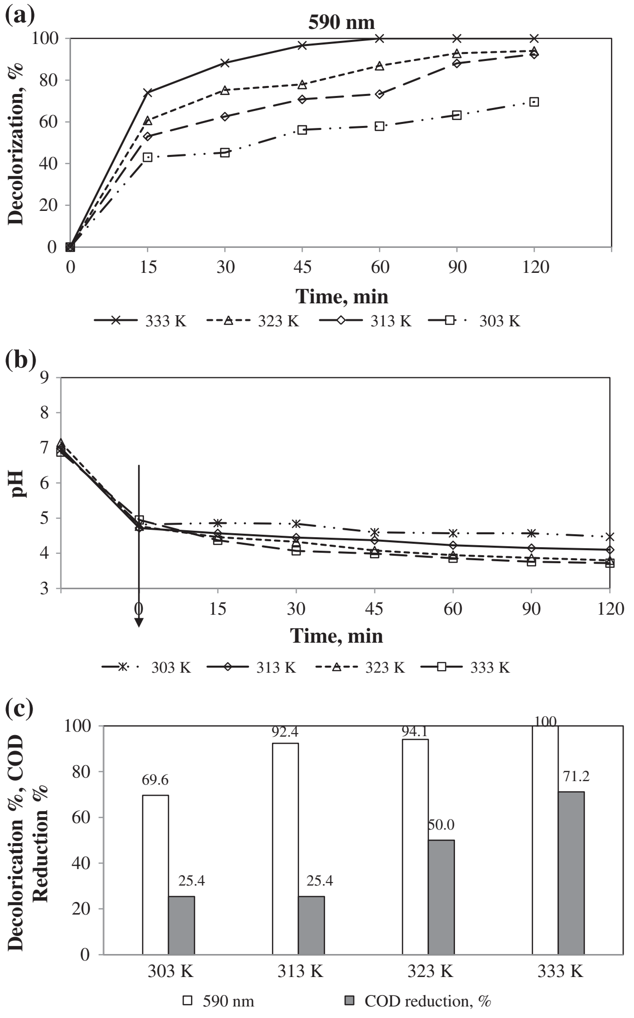

Fig. 10. Catalytic oxidation runs at different temperatures at initial pH around 7.0. (a) Percentage of decolorization as a function of time, (b) pH change as a function of time, and (c) percentage of color removal and COD Reduction after 2 h (0.025 g/dm^3 and 0.15 dm^3 CV solution, 0.15 g catalyst, and 7.5 mM H_2O_2 addition).

results indicated that the presence of iron oxide-coated granular activated carbon (FeGAC) greatly improved the oxidative ability of H_2O_2 for the removal of CV. The removal efficiencies of H_2O_2, GAC, FeGAC, GAC/H_2O_2, and FeGAC/H_2O_2 processes were 10, 44, 40, 43, and 71%, respectively, at room temperature.

In a study done by Fan et al. [10], the homogeneous Fenton reaction of CV was investigated in the presence of $FeSO_4.7H_2O$ or $Fe(NO_3)_3.9H_2O$ as an Fe^{2+} or Fe^{3+} sources, respectively, and the intermediates of the process were identified. Almost complete color removal and 85% TOC removal were obtained after a reaction time of 30 min at room temperature. A 91.9% TOC removal was measured in 1 h by the homogeneous Fenton-like oxidation of CV.

3.2.6. Effect of catalyst stability on catalytic activity

The stability experiments were carried out under the following conditions: 150 mL of 0.025 g/dm^3 CV aqueous solution, 0.15 dm^3 of FeZSM-5 (42) catalyst, 7.5 mM of H_2O_2, 323 K of temperature, and an initial pH of 7.0. The first run was performed with the fresh catalyst (first cycle). To recover the catalyst, after 2 h of oxidation, the final effluent was filtrated and washed with water and then with ethanol. The catalyst was then calcined at 873 K for 2 h and tested in the oxidation of CV (second cycle). After 2 h of reaction, the catalyst was recovered as mentioned above and it was again tested in the oxidation of CV (third cycle). Their performances reached in terms of CV decolorization, and COD removals are presented in Fig. 11. After 2 h of oxidation the color removal was measured as 94.1, 99.3, and 97.8%, respectively. The significant change in color removal observed with the used catalyst may arise from the improvement in surface area and in the

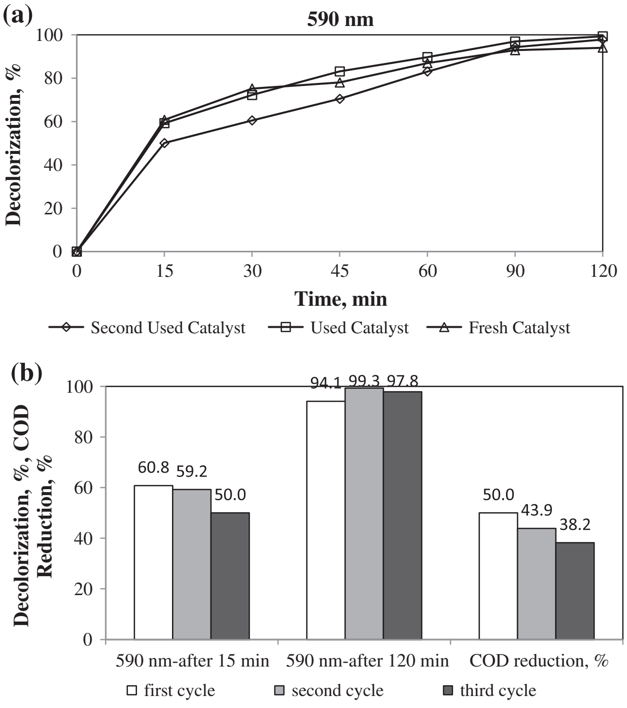

Fig. 11. Stability of the catalyst in the oxidation of CV at an initial pH of 7.0 (a) percentage of decolorization as a function of time and (b) percentage of color removal, and COD reduction after 2 h.

pore size distribution of the catalyst due to the calcination process applied. However, COD removal after 2 h of oxidation decreased from 50 to 43.9% in the second cycle and to 38.2% in the third cycle. No significant change was observed in the solution pH with regard to the reaction time during the three cycles.

The stability of the catalyst was also tested by measuring the iron leaching to the solution. In all the runs, the iron leaching to the solution remained in the range of 0.005–1.0 mg/dm^3 (0.12–2.37%) which is well below EU directives (<2 mg/dm^3) [41]. This small amount of iron leaching shows that the catalyst was stable under the experimental conditions used in this study.

3.2.7. Decolorization kinetics of heterogeneous Fenton-like oxidation of CV

In the oxidation experiments, the reaction mixture was stirred vigorously, thus eliminating the external diffusion resistance between the bulk solution and the catalyst surface. The internal diffusion resistance was also negligible due to the small size of the catalyst particles used in the runs.

The decolorization kinetics of CV was determined for the initial rate.

The initial rate ($-r_{A0}$) can be written as shown in Eq. (7) with an order of m with respect to the initial dye concentration and with an order of n with respect to the initial concentration of H_2O_2.

$$-r_{Ao} = kC^{m}_{CV,o}C^{n}_{H_2O_2,0} \quad (9)$$

When a graph of ln ($-r_{Ao}$) values vs. ln ($C_{CV,o}$) values is plotted for the constant initial concentration of H_2O_2 (7.5 mM) at constant temperature (323 K), the slope of the straight line obtained gives the reaction order (m) with respect to the initial concentration of dye. Fig. 12 displays this relationship. As seen, m is equal to 0.7. From the slope of the straight line obtained from the plot of ln ($-r_{Ao}$) values vs. ln ($C_{H_2O_2,0}$) at a constant temperature (323 K) for the constant initial concentration of dye (0.025 g/dm^3), reaction order (n) with respect to the initial concentration of H_2O_2 is obtained. Fig. 13 presents this plot. As seen, n is equal to 1.

Using the experimental data at different temperatures (Fig. 10(a)), corresponding k values are determined.

According to the Arrhenius equation, ($k = Ae^{-E/RT}$, where A is frequency and R is universal gas constant (8.314 J/mol K)), activation energy (E) is calculated.

Fig. 14 shows ln k vs. $1/T$ dependence. The slope of the straight line is equal to $-E/R$ and E is calculated to be 14.7 kJ/mol.

So, the initial decolorization rate of crystal violet can be written as:

$-r_{CV,o} = 7.3\ e^{-14.7/RT}C_{CV,o}{}^{0.7}\ C_{H_2O_2,0}$

where $C_{CV,o}$ and $C_{H_2O_2,0}$ are in mol/dm^3

Salem [6] determined the activation energy to be 29 kJ/mol in the oxidation of CV with H_2O_2 catalyzed by Amberlyst-15 resin supported with Cu^{2+}-complexes.

In literature on dye degradation by several AOPs, the activation energy of the degradation of Orange II was found to be 17.3 kJ/mol over MnO_2 nanorods at a pH of 2 [68]. An activation energy of 35.9 kJ/mol was reported by Fan et al. [10] in the decolorization of methylorange dissolved in water by nanoscale zerovalent iron particles.

Bolova et al. [36] found the apparent activation energy to be 38.4 kJ/mol for the degradation of Orange II by catalytic wet peroxide oxidation reaction over an iron-loaded ZSM-5 zeolite catalyst.

The activation energy obtained in this study for the degradation of CV is close to the one found by Sun et al. [68].

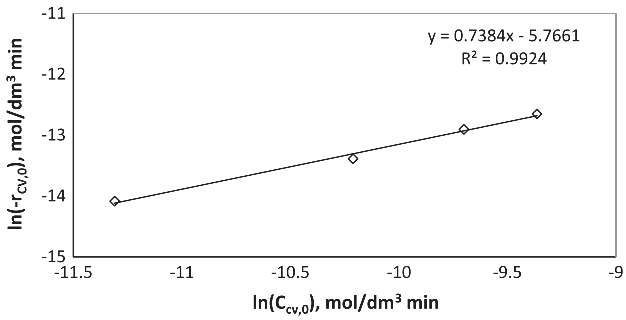

Fig. 12. Graph of ln ($-r_{CV,o}$) values vs. ln ($C_{CV,o}$) values.

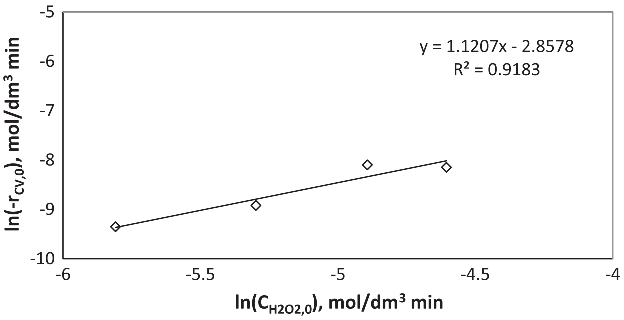

Fig. 13. Graph of ln ($-r_{CV,o}$) values vs. ln ($C_{H_2O_2,0}$) values.

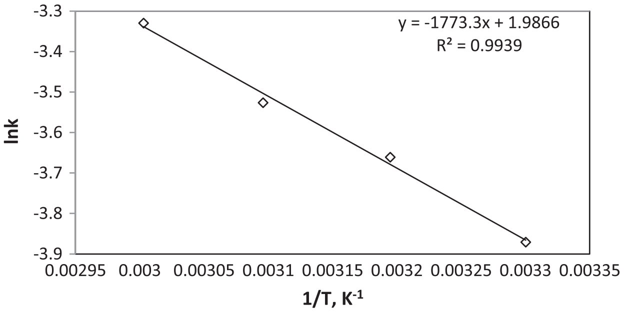

Fig. 14. Graph of ln *k* values vs. 1/*T* values.

4. Conclusions

In this study, the heterogeneous Fenton-like oxidation of CV was investigated in the presence of an iron-loaded ZSM-5 zeolite catalyst. The iron-loaded ZSM-5 zeolite catalyst acted as an efficient and stable catalyst for this process. Complete color removal was obtained in 1 h, and a COD reduction of 71% was achieved after 2 h of reaction with 7.5 mM H_2O_2 at 333 K at dye pH for 0.025 g/dm^3 of CV solution. In all the runs, iron leaching into the solution remained in the range of 0.005–1.0 mg/dm^3 which is well below EU directives (<2 mg/dm^3). This small amount of iron leaching showed that the reaction proceeded under genuine heterogeneous conditions. It can be said that the heterogeneous Fenton-like oxidation process in the presence of iron-loaded ZSM-5 zeolite seems to be an efficient process for dye removal from textile wastewater.

Acknowledgment

The authors acknowledge the financial support from the Ege University Scientific Research Fund under project No. 12 MÜH038.

References

[1] S. Jana, M.K. Purkait, K. Mohanty, Removal of crystal violet by advanced oxidation and microfiltration, Appl. Surf. Sci. 50 (2010) 337–341.

[2] T. Robinson, G. McMullan, R. Marchant, P. Nigam, Remediation of dyes in textile effluent: A critical review on current treatment technologies with a proposed alternative, Bioresour. Technol. 77 (2001) 247–255.

[3] Y.M. Slokar, A.M. Le Marechal, Methods of decolorization of textile wastewaters, Dyes Pigm. 37(4) (1998) 335–356.

[4] C. Sahoo, A.K. Gupta, A. Pal, Photocatalytic degradation of crystal violet (C.I. basic violet 3) on silver ion doped TiO_2, Dyes Pigm. 66 (2005) 189–196.

[5] M.A. Shouman, S.A. Khedr, A.A. Attia, Basic dye adsorption on low cost biopolymer: Kinetic and equilibrium studies, J. Appl. Chem. 2 (2012) 27–36.

[6] I.A. Salem, Activation of H_2O_2 by Amberlyst-15 resin supported with copper (II)-complexes towards oxidation of crystal violet, Chemosphere 44 (2001) 1109–1119.

[7] S. Senthilkumaar, K. Porkodi, Heterogeneous photocatalytic decomposition of crystal violet in UV-illuminated sol–gel derived nanocrystalline TiO_2 suspensions, J. Colloid Interface Sci. 288 (2005) 184–189.

[8] A.K. Gupta, A. Pal, C. Sahoo, Photocatalytic degradation of a mixture of crystal violet (basic violet 3) and methyl red dye in aqueous suspensions using AgC doped TiO_2, Dyes Pigm. 69 (2006) 224–232.

[9] F.A. Alshamsi, A.S. Albadwawi, M.M. Alnuaimi, M.A. Rauf, S.S. Ashraf, Comparative efficiencies of the degradation of crystal violet using UV/hydrogen peroxide and Fenton's reagent, Dyes Pigm. 74 (2007) 283–287.

[10] H. Fan, S. Huang, W. Chung, J. Jan, W. Lin, C. Chen, Degradation pathways of crystal violet by Fenton and Fenton-like systems: Condition optimization and intermediate separation and identification, J. Hazard. Mater. 171 (2009) 1032–1044.

[11] A. Nezamzadeh-Ejhieh, Z. Banan, A comparison between the efficiency of CdS nanoparticles/zeolite A and CdO/zeolite A as catalysts in photodecolorization of crystal violet, Desalination 279 (2011) 146–151.

[12] A. Nezamzadeh-Ejhieh, Z. Banan, Sunlight assisted photodecolorization of crystal violet catalyzed by CdS nanoparticles embedded on zeolite A, Desalination 284 (2012) 157–166.

[13] Y. Ju, J. Fang, X. Liu, Z. Xu, X. Ren, C. Sun, S. Yang, Q. Ren, Y. Ding, K. Yu, L. Wang, Z. Wei, Photodegradation of crystal violet in TiO_2 suspensions using UV-vis irradiation from two microwave-powered electrodeless discharge lamps (EDL$_{-2}$), products, mechanism and feasibility, J. Hazard. Mater. 185 (2011) 1489–1498.

[14] R.E. Palma-Goyes, F.L. Guzman-Duque, G. Peñuela, I. González, J.L. Nava, R.A. Torres-Palma, Electrochemical degradation of crystal violet with BDD electrodes: Effect of electrochemical parameters and identification of organic by-products, Chemosphere 81 (2010) 26–32.

[15] H. Zhang, J. Wu, Z. Wang, D. Zhang, Electrochemical oxidation of crystal violet in the presence of hydrogen peroxide, J. Chem. Technol. Biotechnol. 85 (2010) 1436–1444.

[16] P. Durango-Usuga, F. Guzman-Duque, R. Mosteo, M.V. Vazquez, G. Penuela, R.A. Torres-Palma, Experimental design approach applied to the elimination of crystal violet in water by electrocoagulation with Fe or Al electrodes, J. Hazard. Mater. 179 (2010) 120–126.

[17] C. Chen, W. Chen, M. Chiou, S. Chen, Y. Chen, H. Fan, Degradation of crystal violet by an $FeGAC/H_2O_2$ process, J. Hazard. Mater. 196 (2011) 420–425.

[18] H. Chen, S. Yang, J. Chang, K. Yu, D. Li, C. Sun, A. Li, Efficient degradation of crystal violet in magnetic $CuFe_2O_4$ aqueous solution coupled with microwave radiation, Chemosphere 89 (2012) 185–189.

[19] C. Chen, J. Kuo, H. Yang, Y. Chung, A coupled biological and photocatalysis pretreatment system for the removal

of crystal violet from wastewater, Chemosphere 92 (2013) 695–701.

[20] A. Habib, M. Muslim, T. Shahadat, N. Islam, I.M.I. Ismail, T.S.A. Islam, A.J. Mahmood, Photocatalytic decolorization of crystal violet in aqueous nano-ZnO suspension under visible light irradiation, J. Nanostruct. Chem. 3 (2013) 1–10.

[21] Y. Chen, K. Wang, L. Lou, Photodegradation of dye pollutants on silica gel supported TiO_2 particles under visible light irradiation, J. Photochem. Photobiol. A 163 (2004) 281–287.

[22] K. Dutta, S. Mukhopadhyay, S. Bhattacharjee, B. Chaudhuri, Chemical oxidation of methylene blue using a Fenton-like reaction, J. Hazard. Mater. B84 (2001) 57–71.

[23] F. Torrades, J. Garcia-Montano, J.A. Garcia-Hortal, L. Nunez, X. Domenech, J. Peral, Decolorization and mineralization of homo- and hetero-bireactive dyes under Fenton and photo-Fenton conditions, Color. Technol. 120 (2004) 188–194.

[24] A.M.F.M. Guedes, L.M.P. Madeira, R.A.R. Boaventura, C.A.V. Costa, Fenton oxidation of cork cooking wastewater overall kinetic analysis, Water Res. 37 (2003) 3061–3069.

[25] I.V. Stolyarova, I.B. Kovban, R.V. Prikhod'ko, A.O. Kushko, M.V. Sychev, V.V. Goncharuk, Relationship between the catalytic behavior of ZSM-5 zeolites in oxidative degradation of dyes and nature of their active centers, Russ. J. Appl. Chem. 80(5) (2007) 746–753.

[26] K. Pirkanniemi, M. Sillanpaa, Heterogeneous water phase catalysis as an environmental application: A review, Chemosphere 48 (2002) 1047–1060.

[27] S. Fukuchi, R. Nishimoto, M. Fukushima, Q. Zhu, Effects of reducing agents on the degradation of 2, 4, 6-tribromophenol in a heterogeneous Fenton-like system with an iron-loaded natural zeolite, Appl. Catal. B 147 (2014) 411–419.

[28] R. Gonzalez-Olmos, M.J. Martin, A. Georgi, F.-D. Kopinke, I. Oller, S. Malato, Fe-zeolites as heterogeneous catalysts in solar Fenton-like reactions at neutral pH, Appl. Catal. B 125 (2012) 51–58.

[29] M. Fukushima, K. Tatsumi, Degradation parthways of pentachlorophenol by photo-Fenton systems in the presence of iron (III), humic acid, and hydrogen peroxide, Environ. Sci. Technol. 35 (2001) 1771–1778.

[30] M. Fukushima, K. Tatsumi, K. Morimoto, The fate of aniline after a photo-fenton reaction in an aqueous system containing iron(iii), humic acid, and hydrogen peroxide, Environ. Sci. Technol. 34 (2000) 2006–2013.

[31] K. Fajerwerg, H. Debellefontaine, Wet oxidation of phenol by hydrogen peroxide using heterogeneous catalysis FeZSM-5: A promising catalyst, Appl. Catal. B 10 (1996) L229–L235.

[32] N.H. Phu, T.T.K. Hoa, N.V. Tan, H.V. Thang, P.L. Ha, Characterization and activity of Fe-ZSM-5 catalysts for the total oxidation of phenol in aqueous solutions, Appl. Catal. B 34 (2001) 267–275.

[33] G. Centi, S. Perathoner, T. Torre, M.G. Verduna, Catalytic wet oxidation with H_2O_2 of carboxylic acids on homogeneous and heterogeneous Fenton-type catalysts, Catal. Today 55 (2000) 61–69.

[34] E.V. Kuznetsova, E.N. Savinov, L.A. Vostrikova, V.N. Parmon, Heterogeneous catalysis in the Fenton-type system FeZSM-5/H_2O_2, Appl. Catal. B 51 (2004) 165–170.

[35] E. Bolova, G. Gündüz, M. Dükkancı, S. Yılmaz, Y.C. Yaman, Fe Containing ZSM-5 zeolite as catalyst for wet peroxide oxidation of Orange II, Int. J. Chem. Reactor Eng., 9 Note S1 (2011) 1–20.

[36] E. Bolova, G. Gündüz, M. Dükkancı, Heterogeneous Fenton-like degradation of orange II in water using FeZSM-5 zeolite catalyst, Int. J. Chem. Reactor Eng., 10 Article A 18 (2012) 1–21.

[37] F. Duarte, L.M. Madeıra, Azo-dye Orange II degradation by Fenton's reaction using Fe/ZSM-5 zeolite as catalyst, 2nd European Conference on Environmental Applications of Advanced Oxidation Processes, EAAOP2, 09-11 September 2009, Nicosia, Cyprus.

[38] A. Chen, X. Ma, H. Sun, Decolorization of KN-R catalyzed by Fe-containing Y and ZSM-5 zeolites, J. Hazard. Mater. 156 (2008) 568–575.

[39] M. Dükkancı, G. Gündüz, S. Yılmaz, Y.C. Yaman, R.V. Prikhod'ko, I.V. Stolyarova, Characterization and catalytic activity of CuFeZSM-5 catalysts for oxidative degradation of Rhodamine 6G in aqueous solutions, Appl. Catal. B 95 (2010) 270–278.

[40] M. Dükkancı, G. Gündüz, S. Yılmaz, R.V. Prihod'ko, Heterogeneous Fenton-like degradation of rhodamine 6G in water using CuFeZSM-5 zeolite catalyst prepared by hydrothermal synthesis, J. Hazard. Mater. 181 (2010) 343–350.

[41] N. Demir, G. Gündüz, M. Dükkancı, Degradation of a textile dye, Rhodamine 6G (Rh6G), by heterogeneous sonophotoFenton process in the presence of Fe-containing TiO_2 catalysts, Environ. Sci. Pollut. Res. 22 (2015) 3193–3201.

[42] R. Prihod'ko, I. Stolyarova, G. Gunduz, O. Taran, S. Yashnik, V. Parmon, V. Goncharuk, Fe-exchanged zeolites as materials for catalytic wet peroxide oxidation. Degradation of Rodamine G dye, Appl. Catal. B 104 (2011) 201–210.

[43] Y.C. Yaman, G. Gündüz, M. Dükkancı, Degradation of CI Reactive Red 141 by heterogeneous Fenton-like process over iron-containing ZSM-5 zeolites, Color. Technol. 129 (2013) 69–75.

[44] A.N. Nikolopoulos, O. Igglessi-Markopoulou, N. Papayannakos, Ultrasound assisted catalytic wet peroxide oxidation of phenol: kinetics and intraparticle diffusion effects, Ultrason. Sonochem. 13 (2006) 92–97.

[45] M. Schwidder, M.S. Kumar, K. Klementiev, M.M. Pohl, A. Brückner, W. Grünert, Selective reduction of NO with Fe-ZSM-5 catalysts of low Fe content I. Relations between active site structure and catalytic performance, J. Catal. 231 (2005) 314–330.

[46] F. Heinrich, C. Schmidt, E. Löffler, M. Menzel, W. Grünert, Fe-ZSM-5 catalysts for the selective reduction of NO by isobutane-the problem of active sites, J. Catal. 212 (2002) 157–172.

[47] M.M. Mohamed, I.O. Ali, N.A. Eissa, Effect of thermal treatment on surface and bulk properties of Fe/ZSM-5 zeolites prepared by different methods, Microporous Mesoporous Mater. 87 (2005) 93–102.

[48] Y. Cheng, L.-J. Wang, J.-S. Li, Y.-C. Yang, X.-Y. Sun, Preparation and characterization of nanosized ZSM-5 zeolites in the absence of organic template, Mater Lett. 59 (2005) 3427–3430.

[49] C.P. Nicolaides, A novel family of solid acid catalysts: substantially amorphous or partially crystalline zeolitic materials, Appl. Catal. A 185 (1999) 211–217.

[50] M.S. Batista, M.A. Morales, E. Baggio-Saitovich, E.A. Urquieta-Gonzalez, Iron species present in Fe/ZSM-5 catalysts-influence of the preparation method, Hyperfine Interact. 134 (2001) 161–166.

[51] K. Klier, R.G. Herman, Z. Sojka, J.I. Dicosimo, S. Detavernier, Methane Oxidation Over Dual Redox Catalysts, Final Report, Lehigh University, Bethlehem, 1992, p. 51.

[52] A. Nezamzadeh-Ejhieh, A. Badri, Surfactant modified ZSM-5 zeolite as an active component of membrane electrode towards thiocyanate, Desalination 281 (2011) 248–256.

[53] A. Nezamzadeh-Ejhieh, Z. Shams-Ghahfarokhi, Photodegradation of methyl green by nickel-dimethylglyoxime/ZSM-5 zeolite as a heterogeneous catalyst, J. Chem., ID:104093 (2013) 11.

[54] R. Szostak, V. Nair, T.L. Thomas, Incorporation and stability of iron in molecular-sieve structures. Ferrisilicate analogues of zeolite ZSM-5, J. Chem. Soc., Faraday Trans. 1(83) (1987) 487–494.

[55] A. Nezamzadeh-Ejhieh, M. Karimi-Shamsabadi, Decoloriztion of a binary azo dyes mixture using CuO incorporated nanozeolite-X as a heterogeneous catalyst and solar irradiation, Chem. Eng. J. 228 (2013) 631–641.

[56] A. Nezamzadeh-Ejhieh, M. Amiri, CuO supported clinoptilolite towards solar photocatalytic degradation of p-aminophenol, Powder Technol. 235 (2013) 279–288.

[57] E.E. Ebrahiem, M.N. Al-Maghrabi, A.R. Mobarki, Removal of organic pollutants from industrial wastewater by applying photo-Fenton oxidation technology, Arabian J. Chem. (in press), doi: 10.1016/j.arabjc.2013.06.012.

[58] H.A.A. Medien, S.M.E. Khalil, Kinetics of the oxidative decolorization of some organic dyes utilizing Fenton-like reaction in water, J. King Saud University (Science) 22 (2010) 147–153.

[59] S. Hashemian, M. Tabatabaee, M. Gafari, Fenton oxidation of methyl violet in aqueous solution, J. Chem. 2013 (2013) 1–6 (Article ID 509097).

[60] M. Neamtu, C. Zaharia, C. Catrinescu, A. Yediler, M. Macoveanu, A. Kettrup, Fe-exchanged Y zeolite as catalyst for wet peroxide oxidation of reactive azo dye Procion Marine H-EXL, Appl. Catal. B 48 (2004) 287–294.

[61] http://en.wikipedia.org/wiki/Crystal_violet, January 2015.

[62] A. Adak, M. Bandyopadhyay, A. Pal, Removal of crystal violet dye from wastewater by surfactant-modified alumina, Sep. Purif. Technol. 44 (2005) 139–144.

[63] G.O. El-Sayed, Removal of methylene blue and crystal violet from aqueous solutions by palm kernel fiber, Desalination 272 (2011) 225–232.

[64] A. Nezamzadeh-Ejhieh, A. Shirzadi, Enhancement of the photocatalytic activity of ferrous oxide by doping onto the nano-clinoptilolite particles towards photodegradation of tetracycline, Chemosphere 107 (2014) 136–144.

[65] A. Nezamzadeh-Ejhieh, M. Karimi-Shamsabadi, Comparison of photocatalytic efficiency of supported CuO onto micro and nano particles of zeolite X in photodecolorization of methylene blue and methyl orange aqueous mixture, Appl. catal. A 477 (2014) 83–92.

[66] A. Nezamzadeh-Ejhieh, M. Khorsandi, A comparison between the heterogeneous photodecolorization of an azo dye using Ni/P zeolite zeolite catalyst, Iran. J. Catal. 1(2) (2011) 99–104.

[67] A. Nezamzadeh-Ejhieh, M. Khorsandi, Photodecolorization of eriochrome balck T using NiS-P zeolite as a heterogeneous catalyst, J. Hazard. Mater. 176 (2010) 629–637.

[68] H. Sun, H. Chen, D. Shu, Z. Xie, C. He, L. Peng, Study on degradation of acid orange II in aqueous solution using one-dimensional MnO_2 nanorods, Water Sci. Technol. 61 (2010) 1995–2001.